

Threshold loss of discontinuous permafrost and landscape evolution

LAURA CHASMER and CHRIS HOPKINSON

Department of Geography, University of Lethbridge, Lethbridge, AB T1K 3M4, Canada

Abstract

This study demonstrates linkages between the 1997/1998 El Niño/Southern Oscillation index and a threshold shift to increased permafrost loss within a southern Taiga Plains watershed, Northwest Territories, Canada. Three-dimensional contraction of permafrost plateaus and changes in vegetation structural characteristics are determined from multitemporal airborne Light Detection And Ranging (LiDAR) surveys in 2008, 2011 and 2015. Morphological changes in permafrost cover are compared with optical image analogues from 1970, 1977, 2000 and 2008 and time-series hydro-climate data. Results demonstrate that significant changes in air temperature, precipitation, runoff and a shortening of the snow-covered season by 35 days (1998–2014) and 50 days (1998 only) occurred after 1997. The albedo reduction associated with 35 and 50 days less snow cover leads to increases in shortwave energy receipt during the active thaw period of ~12% (3% annually) and ~16% (5% annually), respectively. From 2000 to 2015, sporadic permafrost loss accelerated from 0.19% (of total basin area) per year between 1970 and 2000 to 0.58% per year from 2000 to 2015, with a projected total loss of permafrost by ~2044. From ~1997 to 2011, we observe a corresponding shift to increased runoff ratio. However, observed increases in the proportion of snow precipitation and the volumetric contribution of permafrost loss to runoff post-1997 (0.6–6.4% per year) cannot fully explain this shift. This suggests increases in drainage efficiency and possible losses from long-term groundwater storage as a result of subtle terrain morphological and soil zone hydraulic conductivity changes. These hydrological changes appear coincident with high vegetation mortality at plateau margins combined with succession-related canopy growth in some bog and fen areas, which are presumed to be drying. Similar changes in runoff response were observed at adjacent Birch, Trout and Jean Marie River watersheds indicating that observations are representative of northern Boreal sporadic permafrost/wetland watersheds in the Taiga Plains.

Keywords: boreal, climate change, ENSO, hydrology, light detection and ranging, permafrost, remote sensing, tipping point

Received 2 September 2016 and accepted 27 September 2016

Introduction

Increasing air temperature over the last few decades in north-western Canada and Alaska has received considerable attention (Serreze *et al.*, 2000) and has been linked to mid-summer forest ecosystem decline within central boreal regions (Goetz *et al.*, 2005; de Jong *et al.*, 2012; Helbig *et al.*, 2016a,b), and large-scale changes in land surface hydrology (Walvoord & Striegl, 2007; St Jacques & Sauchyn, 2009; Walvoord *et al.*, 2012). Loss of productivity and land cover conversion may result in significant feedbacks to the climate system, especially in the form of increased greenhouse gas emissions from previously frozen soils and peatlands (Moore *et al.*, 1998; Turetsky *et al.*, 2002; Tarnocai, 2009; Lara *et al.*, 2015; Helbig *et al.*, in press) and changes in energy balance, which could

exacerbate (Chapin *et al.* 2000) or reduce (Helbig *et al.*, 2016a) northern climate change.

Increases in air temperature and prolonged warming trends in recent years have occurred coincident with the positive mode of several low frequency, ocean-atmospheric teleconnection patterns through the 1970–2000 period. The positive (warm) phase of the Pacific Decadal Oscillation (PDO) began during the mid-1970s and typically lasts for ~30 years before switching into the cooler negative phase (Bonsal & Shabbar, 2011). During the 1980s, air temperature variability was also influenced by frequent positive (warming) modes of the North Atlantic Oscillation (NAO) and increased prevalence of the Southern Oscillation (the atmospheric part of El Niño, ENSO). When combined with the NAO, ENSO accounted for almost half of Northern Hemisphere air temperature variability in winter (Hurrell, 1996). The compounding influence of these patterns results in warmer air temperatures and fewer cold periods in western Canada (Gershunov & Barnett,

Correspondence: Laura Chasmer, tel. +1 403 332 4661, fax +1-403-332 4039, e-mail: laura.chasmer@uleth.ca and Chris Hopkinson, tel. +1 403 332 4586, fax +1 403 332 4039, e-mail: c.hopkinson@uleth.ca

1998; Bonsal *et al.*, 2001; Fleming & Whitfield, 2010), earlier onset of spring (Bonsal & Prowse, 2003), earlier snow melt (Smith *et al.*, 2005; Stewart *et al.*, 2005; DeBeer *et al.*, 2015) and increased runoff from non-coastal rivers (St Jacques & Sauchyn, 2009; Walvoord *et al.*, 2012).

The increased prevalence of these patterns and general climate warming in north-western Canada have had a significant impact on the resilience of many northern boreal permafrost ecosystems. Permafrost underlays approximately 40% of the boreal region (Natural Resources Canada, 2011; Price *et al.*, 2013). Permafrost found in central boreal regions of western Canada is characterized by slightly upraised (0.5–1.0 m), tree (*Picea mariana*) covered permafrost plateaus that overlay frozen peat lenses extending to depths of up to and >10 m (Hayashi *et al.*, 2009). Permafrost plateaus cover 10–50% (sporadic) and 50–90% (discontinuous) of the local land surface area, respectively (Zhang *et al.*, 2003), and are often surrounded by saturated, permafrost-free wetlands with few trees. Perennially frozen soils found within these regions are highly sensitive to small changes in surface energy balance that may result in rapid, complex thaw processes (Camill & Clark, 2000), tree mortality (Baltzer *et al.*, 2014) and non-linear effects on biophysical processes (Jorgenson *et al.*, 2001; Beilman & Robinson, 2003; Quinton *et al.*, 2011). Further, canopy cover and shading (Zoltai & Tarnocai, 1971; Camill & Clark, 2000) exert strong controls on permafrost thaw, such that maintenance and continued growth of trees and understory shrubs will reduce transient permafrost response to warming typically along north-facing plateau margins (Halsey *et al.*, 1995; Camill & Clark, 1998, 2000). The exception to this occurs if and when a threshold (e.g. disturbance) is reached that changes the environmental conditions with which permafrost is maintained (Camill & Clark, 2000).

While there have been references to the effects of the intense ENSO of 1997/1998 on permafrost thaw (Camill, 2005; Smith *et al.*, 2005; Jorgenson *et al.*, 2006), little is known about the trajectories of permafrost degradation since this period, the topographic and canopy characteristics that have either maintained permafrost or exacerbated decline, and the runoff response to permafrost thaw. Further, thermal inertia within permafrost/wetland areas may have created a 'tipping point' scenario with which accelerated thaw continues to degrade relict permafrost. This has forced rapid landscape evolution and succession, such as from plateau forest to saturated wetlands, changing the characteristics of water balance and movement through the watershed (Connon *et al.*, 2014), and potentially altering the net effect of climate feedbacks (Helbig *et al.*,

2016b, in press). Yet, minimal long-term permafrost monitoring data (e.g. Smith *et al.*, 2001), limited availability (and potential error) of meteorological and hydrometric data (Woo & Thorne, 2003), and lags between thaw-induced vegetation mortality and its manifestation in long-term optical remote sensing data (Chasmer *et al.*, 2011) limit our ability to quantify the influence of multiyear climate anomalies on northern ecosystems.

The primary objective of this study is to present quantitative evidence of a threshold change or acceleration in permafrost thaw trajectories and greater runoff response characteristics that occurred following the ENSO anomaly of 1997/1998 within the sporadic to discontinuous permafrost zone of the Northwest Territories, Canada. To do this we: (i) quantify a shift in the runoff response pre- and post-1997/1998; (ii) demonstrate that permafrost loss increased since the 1997/1998 ENSO and examine the volumetric meltwater contribution to basin runoff using multitemporal airborne Light Detection And Ranging (LiDAR); (iii) characterize changes in vegetation structure along plateau and wetland edges that may be indicative of permafrost thaw or resilience; and (iv) identify areas of differential vegetation growth and decline within wetlands that may be associated with changes in drainage efficiency or vegetation succession processes.

Materials and methods

Study area

The Scotty Creek watershed (SCW) (~139 km²) is located within the sporadic to discontinuous permafrost region of the Taiga Plains ecozone, ~50 km south of Fort Simpson in the Northwest Territories, Canada (Fig. 1a) (61.44°N, 121.25°W) (Quinton *et al.*, 2003; Quinton & Baltzer, 2013). The watershed is comprised of a heterogeneous mixture of upland moraines (48%), upraised permafrost-cored plateaus (20%), ombrotrophic bogs (19%), fens (12%), and lakes (2%) (Chasmer *et al.*, 2014; Fig. 1b). The watershed is also relatively undisturbed with no evidence of wildfire in its recorded history (since 1965), with the exception of a small fire south of Goose Lake in 2014 (largest lake in Fig. 1, Government of the NWT, 2016). Historical aerial photography at the site indicates that seismic line development and trail installation have increased since the 1970s (Williams *et al.*, 2013). Runoff from the watershed is monitored at a Water Survey of Canada hydrometric gauging station before draining into the Liard River 60 km upstream of the confluence with the Mackenzie River.

Hydrometric and meteorological data analysis

Historical daily air temperature data (maximum, minimum, and mean) (T_{air}) and cumulative precipitation (P, including rain, snow water equivalent (SWE), and snow depth) were

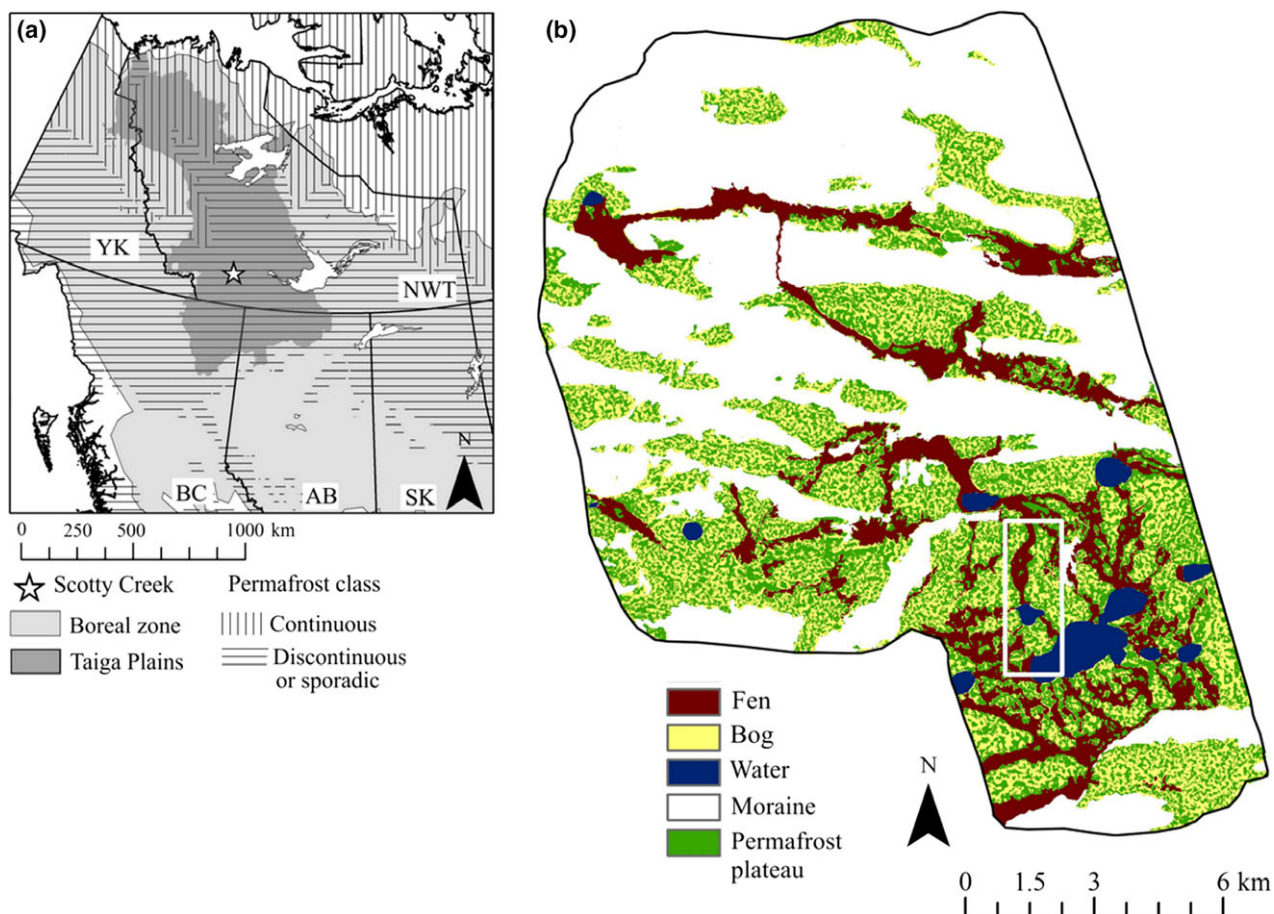


Fig. 1 (a) The location of the SCW study basin within the Taiga Plains ecozone, Northwest Territories, Canada; (b) Land cover classification and approximate boundary described in Chasmer *et al.* (2014) with overlapping LiDAR survey area of interest (AOI) represented by the white rectangle.

acquired for the town of Fort Simpson from 1970 to 2014 (Meteorological Service of Canada, 2016) and resampled to mean T_{air} and cumulative P (snow cover, SWE, depth (including snow depletion curves), and rain) each month and per water year (October to September), warm season (April to October), and cold season (November to March), assuming these represent the climate of SCW (Connon *et al.*, 2014). The onset of sustained snow melt each year was defined as the last day following three consecutive days of $T_{\text{air}} > 0^{\circ}\text{C}$ (Woo & Thorne, 2003). Runoff data (Q) were downloaded from the Water Survey of Canada stream gauge for the SCW (1996–2015) and the adjacent Jean Marie watershed (1973–2015) (Water Survey of Canada, 2016). To extend the runoff period at SCW to approximately match historical remote sensing data, annual variability of areal runoff yield at SCW is compared with that of Jean Marie watershed using a linear regression ($R^2 = 0.97$, $\text{RMSE} = 10\%$) and hindcast to 1973 using the linear model ($Q_{\text{Scotty}} = 0.96 (Q_{\text{Jean Marie}}) - 6.22$). Scotty Creek and Jean Marie watersheds have similar proportions of bog and fen land cover types (Connon *et al.*, 2014). Runoff data from adjacent forested peat plateau-wetland watersheds, Trout (1970–2014) and Birch (1974–2014) as well as Jean Marie

add credibility to the findings based on the shortened/regressed data record at SCW. Runoff ratio (Q/P) provides an index of water partitioning into runoff, after accounting for other losses (evapotranspiration and storage), and is a response mechanism to the combined influences of evapotranspiration, permafrost thaw, and changes in storage. The partitioning of Q into runoff from melting snow at the beginning of the snow season (Q/snow) and the contribution of snow to precipitation (snow/ P) are considered to quantify the changing relative importance of precipitation type and its possible impact on runoff. Significant threshold changes, which we define as timing of shifts in the trend of water year hydro-climatic data, are quantified using a change point analysis (e.g. Killick *et al.*, 2012), bootstrapped 10,000 times to determine the significance of the magnitude and timing of the threshold change.

To estimate the potential effects of changes in the length of the snow-covered period on permafrost thaw, we test a simple energy absorption scenario for SCW using average albedo (α) during snow-covered and snow-free periods. Incoming short-wave radiation ($K\downarrow$, Wm^{-2}) is estimated from solar azimuth and zenith angles at a given latitude for SCW, and including a

constant atmospheric transmissivity for average (uniform) sky conditions (0.5). Total absorbed radiation is estimated as $K\downarrow - K\uparrow = \alpha K\downarrow$, based on an average α of a black spruce covered permafrost plateau in winter of ~0.35, and a maximum open wetland α of 0.85 measured above a treed plateau and a bog at SCW (Helbig *et al.*, 2016a).

Standardized positive and negative anomalies of the PDO (Mantua, 2016) and Southern Oscillation Index (SOI, NOAA, 2016) (inverted such that SOI is positive) were determined by calculating the residual from the long-term mean (44 years) and dividing by the standard deviation (Bonsal & Shabbar, 2011). Variability of climatic (T_{air} , P , snow (SWE)) and hydro-metric data (Q , Q/P , Q/snow , snow/P) measured during the 44-year period are examined during pre-ENSO (1970–1996) and post (1997–2015)-ENSO periods using an analysis of variance to quantify whether or not statistically significant differences between the two periods exist.

Remote sensing data collection and analysis

Discrete return airborne scanning LiDAR surveys were collected by the authors within a 3.6 km \times 1.4 km area of interest (AOI) in the southern part of the watershed (Fig. 1b) during the first two weeks of August in 2008, 2011, and 2015, and for the entire basin in 2010. In 2008, 2010, and 2011, a Teledyne Optech Inc. Airborne Laser Terrain mapper (ALTM) 3100 EA (Toronto, Canada) (Chasmer *et al.*, 2014) was used, while the 2015 data set was acquired with an Optech Aquarius topographic/bathymetric laser mapping system (Hopkinson *et al.*, 2016). Aerial survey control was afforded using a Global Positioning System (GPS) base station located at the Fort Simpson Airport. Additional spectral imagery was also acquired coincident with LiDAR surveys: the 2008 mission captured simultaneous high-resolution digital near infrared (NIR) aerial photography (Chasmer *et al.*, 2011) and in 2011 high-resolution thermal imagery. Laser pulse range, inertial measurement unit and GPS data were integrated and quality controlled and then classified into ground and non-ground returns. Ground returns were gridded to generate 1 m spatial resolution raster digital elevation models (DEMs) for each data set (2008, 2011, and 2015) and then validated for ground surface elevation in 2010 along transects using survey-grade differential GPS at >100 measurement locations near the centre of the AOI (Chasmer *et al.*, 2014). Maximum differences between 2008 and 2015 were determined by subtracting 2008 from 2015 for the AOI to provide aerial quantification of permafrost loss.

The use of two different LiDAR systems may yield slightly higher ground surface elevations in 2015 using the 532 nm Aquarius, on average, compared with surveys in 2008 and 2011 at 1064 nm (near infrared). Hopkinson *et al.* (2016) found a mean difference of 0.07 m (within the range of error of both systems). Further, a slight reduction in the 2015 canopy heights may be attributed to laser pulse attenuation and foliage absorption at 532 nm. Systematic differences are small compared to the differences observed in this study, the implication being that observed growth may be very slightly underestimated and canopy losses very slightly overestimated, but the reported trends are unchanged.

Permafrost area is extrapolated from the AOI to watershed based on proportional land cover for each year of survey. This is then expressed as a percentage of the total area of all land cover types (Chasmer *et al.*, 2014). Plateau classification accuracy compared with *in situ* survey GPS validation transects is 91% (Chasmer *et al.*, 2014). LiDAR classified plateaus in 2008, 2011 and 2015 are compared with manually delineated results obtained from ortho-rectified photogrammetric images collected in 1970 and 1977 (black and white air photos), 2000 (IKONOS satellite imagery), and 2008 (NIR digital air photos) (Chasmer *et al.*, 2011). Spatial differences between plateau and forest areas on a per pixel basis are used to estimate historical plateau area from forest extent in 1970, 1977 and 2000 based on the coincident 2008 digital air photograph and LiDAR DEM, where plateau area is smaller than forested area due to lags in tree mortality associated with permafrost thaw. This assumes that the linear distance between the edge of the canopy and the edge of the plateau is the same when using the 2008 data set to spatially hindcast the plateau extent to 2000, 1977, and 1970. Time-series trends in plateau area decline are compared using linear and quadratic (best fit) regression analysis of plateau area (dependent variable) over time (independent variable), including 95% confidence intervals for the 1970–2015 period. To provide evidence for a threshold change in permafrost thaw during the mid- to late-1990s associated with compounding teleconnection influences, a linear regression model from 1970 to 1977 is linearly forecast to 2000, while regression from 2000 to 2015 is linearly hindcast to 1990.

Volumetric loss of permafrost used to estimate thaw contribution to runoff is determined from 3D pixels (voxels) (x , y , z) based on horizontal contraction and vertical loss between 2008 (t_1) and 2015 (t_2), for areas where plateau vertical loss exceeds 0.2 m over the seven-year period. To determine water equivalent per voxel associated with loss of permafrost, we assume a volumetric frozen water content (VMC) of 0.83 (D. Olefeldt, Personal communication), such that:

$$\left(\left(\frac{\Delta \text{VMC}_{\text{voxel}} \times \text{PA}_{\text{basin}}}{\text{PA}_{\text{AOI}}} \right) A_{\text{basin}} \right) \times 1000, \quad (1)$$

where PA_{basin} is the classified permafrost area of the watershed, PA_{AOI} is the permafrost area found within the AOI (used to determine volumetric loss from LiDAR data), and A_{basin} is the total land surface area of the watershed. The $\times 1000$ multiplier provides an estimate (in mm) of the minimum contribution of melt water input from permafrost loss to basin runoff. To estimate maximum contribution, 10 m (depth) is added per voxel following Hayashi *et al.* (2009) who found that maximum depth of permafrost in the SCW was ~10 m.

Finally, changes in vegetation canopy structural characteristics (tree height and canopy cover) associated with permafrost maintenance and changes in wetland vegetation are also determined between 2008 and 2015 LiDAR data sets. Canopy height models (CHMs) were derived for each year by rasterizing a digital surface model (DSM) of the mean maximum height of laser pulse returns within a 1.5 m search radius (1 m resolution) to maintain the shape and radius of tree structures

and understory vegetation. CHMs were derived using standard methods by subtracting the DEM from the DSM such that heights would be normalized relative to ground level (e.g. Hopkinson *et al.*, 2005). To remove the influence of possible tree stem position change between surveys (as might occur due to wind or as stems begin to lean at plateau margins), mean canopy heights were resampled to 5 m. The change in canopy height was estimated by subtracting the 2008 CHM from that of 2015. Impacts of landscape evolution on the spatial variability of vegetation maintenance or succession are examined along the edges of plateaus and within wetlands. To do this, 5000 pixels containing changes in canopy heights between 2008 and 2015 were randomly selected and subsequently sorted into: (i) north to east [337.5°(N) to 112.5°(NE)] and south to west [157.5°(S) to 292.5°(SW)] facing plateau slopes and areas extending to the extent of permafrost in 1970. This division is used to identify the impacts of variable rates of thaw on tree and shrub maintenance; (ii) *Sphagnum fuscum* mounds within the fen that are slightly topographically elevated compared to the surrounding ground surface; and (iii) depressed fen areas. Distances between randomly sampled points exceeded 5 m to avoid spatial autocorrelation between pixels. Slight undulations in fen ground surface morphology (defined as topographically elevated and depressed compared with surrounding planar surface) were determined using a topographic position index based on localized characteristics of the fen surface. A 45 m low-pass filter is used to identify the general trend of fen surface morphology, subtracted from the high-resolution DEM (Chasmer *et al.*, 2014).

Results

Influence of the 1997/1998 ENSO anomaly on a shift in water balance

Over the last 44 years, the negative phase of the Southern Oscillation Index (SOI) [inverted to compare with the warm, positive mode of the Pacific Decadal Oscillation (PDO)] is aligned with the two-year running average trend of the PDO (Fig. 2a) (e.g. Bonsal & Shabbar, 2011). The negative (cool) phase of the PDO switches into predominantly warm phase during the mid-1970s and is characterized by more frequent and intense El Niño periods before switching to negative phase during the late 2000s. The strong ENSO phase in 1997/1998 was marked by significantly warmer and prolonged mean (and maximum) water year T_{air} , while the 1982/1983 ENSO was 0.9 °C cooler, on average (Fig. 2b). Cumulative snow precipitation decreased throughout the 1970s to the mid-1990s (linear rate of loss of 0.7 mm yr⁻¹ on average, Fig 2c), coinciding with a warm period that started in 1992, and seven years of earlier than average spring snow melt (Fig. 2b). The years between 1990 and 1995 received below-average rain and slightly above average snow, shifting to greater snow accumulation after 1998 (linear rate of gain of 5.7 mm yr⁻¹). To

this end, we concentrate on changes in hydro-climatology and permafrost thaw during and after the 1997/1998 ENSO anomaly.

T_{air} measured at Fort Simpson was 1.7 °C (mean), 1.4 °C (maximum) (1997/1998), and 4.6 °C (mean), 5.3 °C (maximum) (2014/15) warmer than the long-term mean (1971–2015) (Table 1). However, the greatest differences in T_{air} occurred during the cold season, where maximum T_{air} was warmer than the long-term mean by 1.8 °C (1997/1998) and 6.5 °C (2015/2016), indicating that this region, like others in north-western Canada, is experiencing less cold weather (Mantua *et al.*, 1997; Zhang *et al.*, 2000; Bonsal *et al.*, 2001; Shabbar & Bonsal, 2003; Stewart *et al.*, 2005). A significant shift to warmer air temperatures indicated by change point analysis occurred in 1992 ($P = 0.07, 0.02, 0.02$ max. mean and min. T_{air}), and by 1998, T_{air} was above 0 °C eight days earlier in spring and continued 15 days later in autumn compared with the 1971–2014 average.

Warmer T_{air} since the early 1990s and during 1997/1998 corresponds with a 39% increase in snow depth (cm). Decadal snow cover depletion curves between the 1970–1979 and 2000–2009 periods demonstrate a noticeable shift in average snow-covered conditions, 21 days later in autumn during the 2000+ period (October 14th as opposed to September 23rd), and average no-snow conditions 14 days earlier in spring (May 3rd as opposed to May 17th) (for continuous coverage at a depth >1 cm) (Fig. 3). Greater accumulation occurred during the warmer late autumn/early winter period. In 1998, there was 2/3 more snowfall than the long-term (44 year) average. Seasonal start of snow accumulation approximately matched that of 2000–2009 (within one day) and had completely melted by April 18th, 30 and 16 days earlier than the 1970s and 2000s period, respectively (Fig. 3), and 50 days earlier than the average experienced during the 1970s (Fig. 2b).

Rates of areal loss of permafrost pre- and post-1997/1998 ENSO

Connon *et al.* (2014) suggest that permafrost thaw and conversion of plateaus to wetlands between 1970 and 2010 has increased the efficiency with which water moves through the basin. However, it is not known whether the ENSO event of 1997/1998 and associated changes in T_{air} and snow precipitation/timing of snow melt was a catalyst for increased permafrost thaw and runoff efficiency after 1997/1998. Areal rate of permafrost thaw follows a quadratic trend of accelerating loss (Fig. 4a), which is most apparent since the 1997/1998 ENSO. The 95% CI also demonstrates the least model uncertainty using the quadratic fit (Fig. 4a) with lower standard error (S) compared with that of the

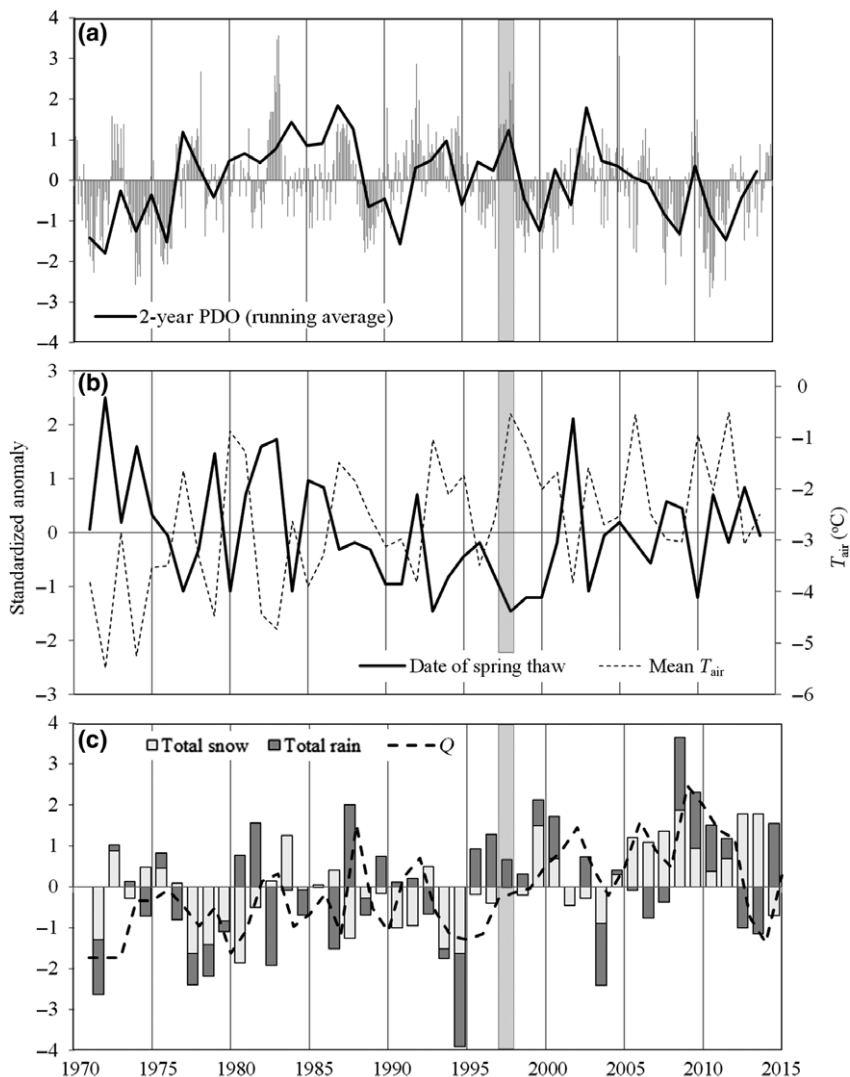


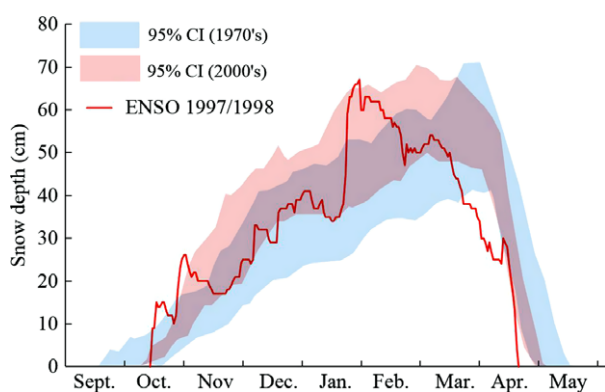
Fig. 2 (a) Standardized anomalies of the Southern Oscillation Index (SOI) (positive bars = El Niño; negative bars = La Niña) and two-year running average Pacific Decadal Oscillation (PDO) illustrating correspondence between positive PDO and ENSO (and vice versa); (b) standardized anomaly of date of spring snow melt where negative = earlier in season and positive = later in season; mean T_{air} ; (c) standardized anomalies of total rain and snow where positive = more rain (and/or snow), negative = less rain (and/or snow), and runoff (Q). Light grey bar in each plot represents the timing of the 1997/1998 ENSO.

linear fit (Fig. 4b). Conservative linear loss from 1970 to 2015 indicates a rate of permafrost loss of 0.34% per year (of total land cover area). Assuming a threshold of accelerated loss from 1997 to 2015 (Fig. 4c), linear losses up to that threshold (1970–1977) are 0.19% per year, (forecast to 2000), and increase to 0.58% per year from 2000 to 2015 (hindcast to 1990). This is equivalent to losses of 0.20 km² per year from 1970 to ~1998, and 0.63 km² per year from ~1999 to 2015, indicating drastic plateau to wetland conversion. Forecast and hindcast linear models intercept in 1997 (Fig. 4c), providing evidence of a potential threshold in the rate of permafrost loss. Caution must be exercised over the exact timing of

the intercept given it relies on a forecast from two historical data points where areal uncertainties are greatest. For example, if we assume an extreme case, where plateau areas in 1970 and 1977 are averaged and projected forwards, we arrive at an intercept of the curves in 1990 (Fig. 4c). However, it is clear from the confidence intervals in Fig. 4c that the trend in the data from 2000 onwards is linear and any shift in the long-term trend must have occurred shortly before 2000. Consequently, the remote sensing-based evidence shows 1990 to 2000 to be the maximum possible range for the timing of a dramatic shift in permafrost loss, with the most likely projections converging on 1997–

Table 1 Summary statistics on water year, warm and cold season T_{air} , P , and Q , including significant differences between periods 1970–1996 (pre-1997/1998 ENSO) and 1997–2015 (including and post-1997/1998 ENSO)

Climate variable	Averaging/cumulative period	1970–1996 (pre-ENSO) average (SD)	1997–2015 (post-ENSO) average (SD)	Ave. residual	P -value
Ave. max. T_{air} ($^{\circ}\text{C}$)	Water year	2.3 (1.2)	3.0 (1.0)	+0.69	0.06
	Cold season	−15.0 (2.0)	−13.1 (2.8)	+1.90	0.01
	Warm season	14.6 (1.1)	15.1 (1.0)	+0.47	0.18
Ave. min T_{air} ($^{\circ}\text{C}$)	Water year	−9.0 (1.2)	−7.6 (1.4)	+1.35	0.001
	Cold season	−25.3 (2.1)	−22.8 (1.9)	+2.45	0.0005
	Warm season	2.58 (0.9)	3.4 (0.1)	+0.85	0.002
Ave. mean T_{air} ($^{\circ}\text{C}$)	Water year	−3.3 (1.2)	−2.3 (1.0)	+1.04	0.005
	Cold season	−20.0 (1.9)	−17.9 (2.3)	+2.18	0.002
	Warm season	8.6 (1.0)	9.3 (1.0)	+0.7	0.08
Total rain (mm)	Water year	218.3 (78.4)	242.3 (67.3)	+24.0	0.04
Total snow (mm)	Water year	160.4 (47.4)	222.5 (53.0)	+62.0	0.0003
Runoff (mm)	Water year	84.6 (53.2)	160.9 (65.3)	+76.3	<0.0001
Runoff ratio (Q/P)	Water year	0.23 (0.1)	0.40 (0.1)	+0.17	<0.0001
Snow/P	Water year	0.44 (0.14)	0.58 (0.17)	+0.14	0.10
Q/snow	Water year	0.53 (0.30)	0.76 (0.35)	+0.22	0.06

**Fig. 3** 95% CI of snow cover depletion curves in the 1970s compared with those of the 2000s for periods where snow cover stays on the ground for four or more days. The 1997/1998 ENSO curve is also included.

98). Given this convergence occurs coincident with observed shifts in hydro-climatological record pre- and post-1997/1998 ENSO (Fig. 2a, b), there is high confidence that this event triggered the acceleration of permafrost loss in the study area. Projecting the post-1997/1998 ENSO linear permafrost loss model forwards suggests a total loss of near-surface permafrost by 2044.

Post-1997/1998 ENSO spatial variability of permafrost contraction and maintenance

The linear projection forwards in time to a no-permafrost state assumes that controls on permafrost maintenance (e.g. Camill & Clark, 2000) will similarly decline following the 1997/1998 ENSO. However, spatial variability in

volumetric plateau contraction between 2008 and 2015 indicates that this is not likely a realistic scenario. Figure 5 illustrates elevation differences between 2008 and 2015 based on LiDAR-derived DEMs. Greatest cumulative losses are preferentially distributed to south and west-facing plateau edges associated with energy inputs from incident solar radiation during midday and afternoon periods. These marginal areas also correspond with significant tree canopy loss associated with permafrost thaw and increased ground saturation (e.g. Baltzer *et al.*, 2014). Average vertical height reduction associated with foliage loss and displaced/tilted and falling trees was 1.1 m (SD = 1.0 m) from 2008 to 2015 (Fig. 6a). On north- to east-facing plateau edges, however, rates of contraction are much lower, indicating that these edges are not exposed to the same drivers of permafrost thaw. In contrast, trees and shrubs along north to east plateau edges indicate little to minimal growth (0.5 m, SD = 0.6), which may be due to vegetation densification, but requires further investigation (Fig. 6a).

Wetlands also underwent successional changes within the 7 years of available LiDAR data. The spatial variability of vegetation growth/densification and loss/defoliation between 2008 and 2015 LiDAR-derived CHMs is illustrated in detail in Fig. 7. The broad fen extending from south to north on the western side of Fig. 7 illustrates 22% areal increase in vegetation densification and growth (where vegetation height changes are >0.2 m) throughout the 2008–2015 period. This indicates that peat conditions have become more favourable for shrub encroachment over this period. Further, growth and/or densification occurs primarily on

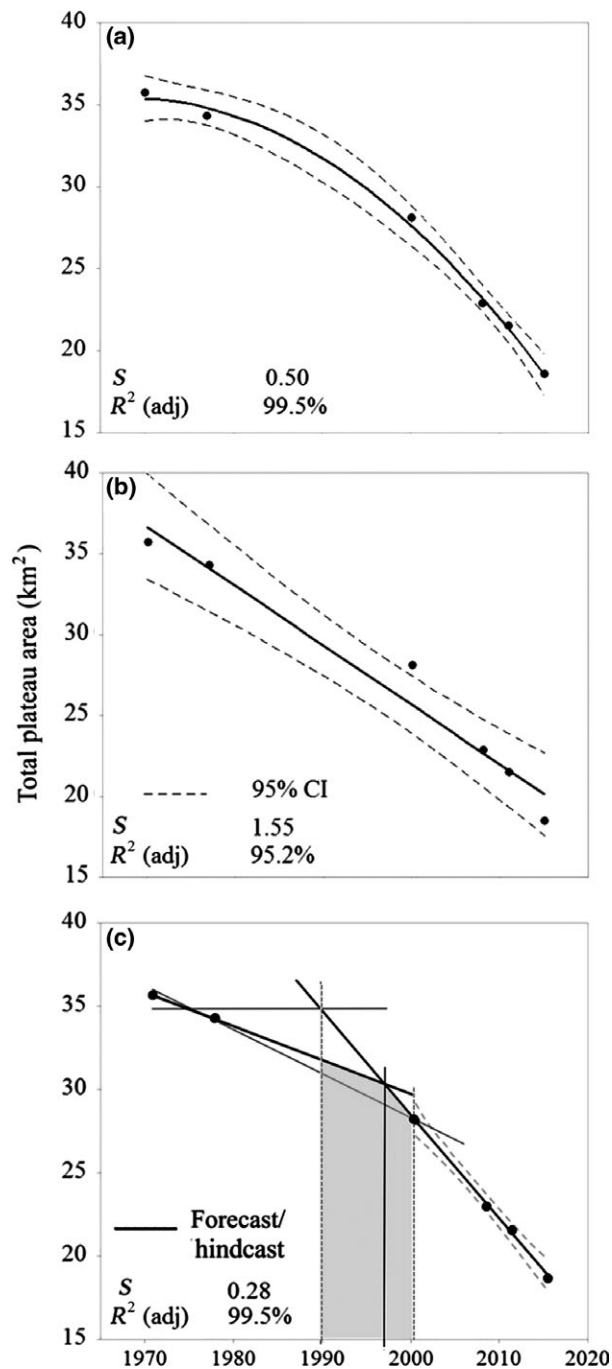


Fig. 4 Accelerating permafrost area decline based on lateral DEM contraction and 95% confidence interval using: (a) a quadratic model, (b) a conservative linear model, and (c) linear models applied from 1970 to 1977 (forecast to 2000) and 2000 to 2015 (hindcast to 1990), with the year of model intercept occurring in 1997 (S refers to standard error). Maximum range of period associated with accelerated thaw (shaded) is bounded by a condition of static plateau area (no loss) from 1970 to 1977 (minimum) and extension of linear thaw from that period to 2000 (maximum).

locally elevated parts of the fen where we observed 0.4 m (SD = 0.6 m) height increase, on average (Fig. 6b). In areas of local topographic depressions within the fen, we find insignificant change in vegetation height (mean = -0.02 m, SD = 0.03 m). This characterizes approximately 13% of the fen (Fig. 6b), and likely represents areas of high moisture content and recently anoxic soil conditions less favourable for growth (Baltzer *et al.*, 2014; Fafard, 2014). Evidently, while parts of the fen have undergone rapid shrub/tree vegetation encroachment and growth, a high proportion of smaller ombrotrophic and connected bogs, especially those that were previously isolated, have experienced loss of vertical vegetation structure (heights <0.2 m = 38% of bog area coverage). Larger, connected bogs >0.7 ha demonstrate a bimodal variability in vegetation change, where one part of the bog is characterized by declining vegetation heights while the other is characterized by vegetation growth and/or densification (~14% of bog areas). These observations of vegetation succession and change may be indicative of increased overall drainage efficiency and associated localized drying and wetting influences over the seven-year period alluded to in Fafard (2014).

Permafrost loss contribution to runoff and changes in drainage efficiency

Accelerated permafrost loss and changes in vegetation structural characteristics are evidence of ecosystem response to shifts in the energy and hydrological regimes within the SCW. Figure 8 illustrates a significant change in the threshold response of runoff ratio (Q/P) that occurred post-1998. Prior to the 1997/1998 ENSO, mean areal runoff was 85 mm yr⁻¹ (SD = 52 mm yr⁻¹) and was almost double that during the period following ENSO (161 mm yr⁻¹, SD = 65 mm yr⁻¹) ($P < 0.0001$) (Table 1). Q/P was relatively stable between 1973 and 1997 (mean Q/P = 0.23; SD = 0.10, $R^2 = 0.01$) but began to trend upwards, increasing by 74% to 0.40 (SD = 0.1; $R^2 = 0.65$) (Table 1, Fig. 8), including abnormally dry years in 2013 and 2014, and a cool year in 2012. Change point analysis indicates that a significant change in direction in Q and Q/P occurred in 1998 ($P = 0.0001$ and 0.0002, respectively), along with similar shifts in Q at Jean Marie, Birch River, Trout River watersheds ($P = 0.0001$, 0.01, and 0.02, respectively). This adds credibility to the short data record and regressed Q (from Jean Marie watershed) at SCW pre-1996. Despite significant increase in cumulative snow precipitation after 1997 [from change point analysis ($P = 0.01$)], and greater proportion of snow/P (~23%

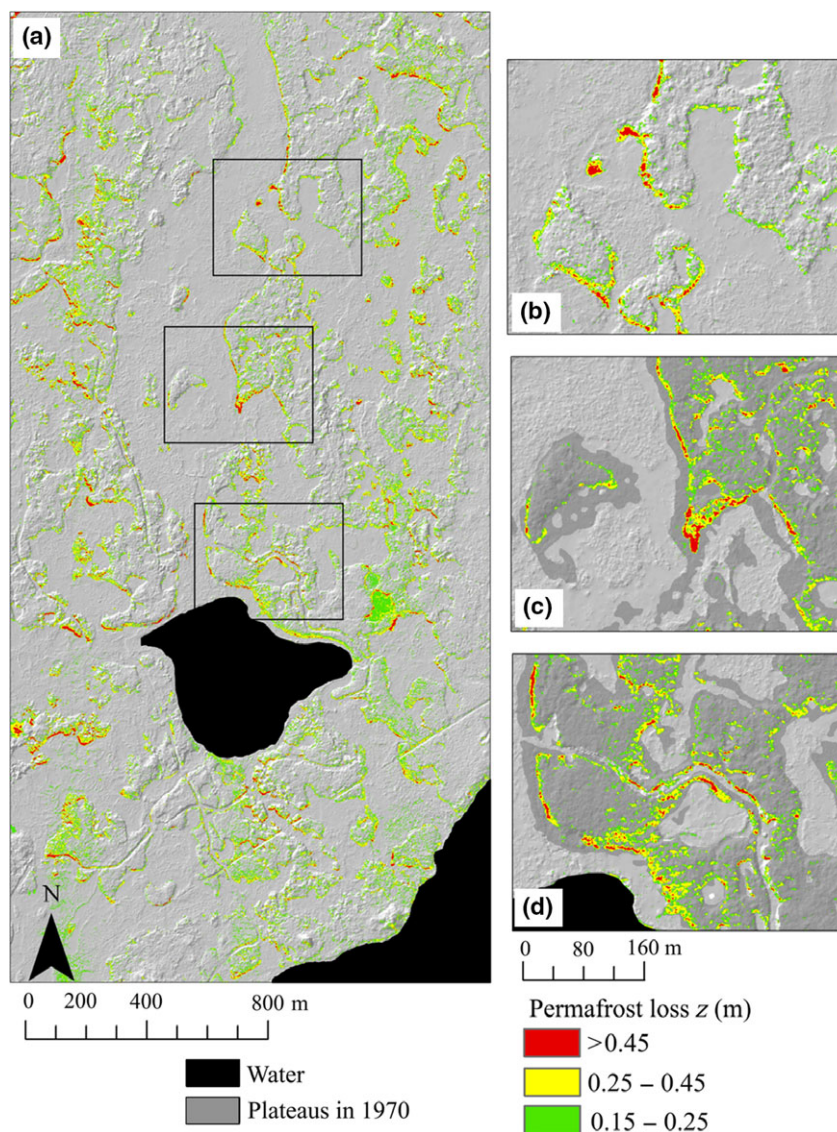


Fig. 5 (a) Terrain surface elevation (z) changes between 2008 and 2015 determined from LiDAR data across the AOI. Inset images (b–d) provide greater detail of permafrost change and contraction at plateau edges. In (c and d), plateau area extent in 1970 is also provided for visual comparison.

since 1997), snow did not contribute enough melt water to explain near doubling of Q and Q/P following ENSO. Average Q/snow increased by $\sim 30\%$, indicating greater losses from Q relative to contribution from snow since 1997 (Table 1). The threshold change in Q/P at SCW therefore approximately coincides with the initiation of accelerated loss of permafrost plateau extent and with moderate contribution from snow melt ($P = 0.01$) (Fig. 4c).

Despite these results, volumetric permafrost loss that occurred from 2008 to 2015 also cannot directly account for the change in basin yield. Basin-wide volumetric loss of plateau area is approximately $9.4 \times 10^3 \text{ m}^3$ per

year. The contribution of permafrost plateau melt water to basin runoff is at minimum 0.6% per year, for thawing permafrost edges above the elevation of proximal wetlands. This increases to an extreme of 6.4% per year, for an estimated maximum permafrost depth of 10 m (Hayashi *et al.*, 2009). Therefore, the contribution of long-term permafrost loss to Q/P varies between 0.4% and 4% (of average runoff between 2008 and 2015), while minimum contribution of permafrost loss to runoff is least during high runoff years (e.g. 2009, $Q = 317 \text{ mm yr}^{-1}$; thaw contribution = $\sim 0.1\%$ to 2% max.) and greatest during low runoff years (e.g. 2014, $Q = 26 \text{ mm yr}^{-1}$; thaw contribution = 2% to 24% max.).

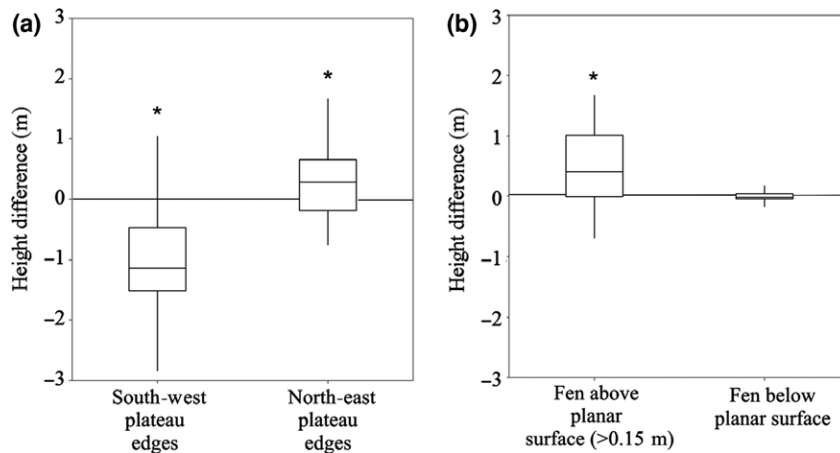


Fig. 6 Differences between canopy height model (CHM) changes from 2008 to 2015 within: (a) historical permafrost edges identified in 1970; and (b) within topographically elevated vs. low-lying fen areas. Box plots illustrate median, interquartile range, 5th and 95th percentiles and median significantly different from zero (asterisk).

Discussion

Links between a hydro-climatic anomaly and threshold behaviour in permafrost loss

The shift to accelerated permafrost loss from 0.19% (1970–1977, forecast to 2000) to 0.58% (2000 to 2015) per year within the basin (Fig. 4c) corresponds with a shift in behaviour of hydro-climatic variables and watershed response occurring around the time of the 1997/1998 ENSO. It therefore follows that changes in permafrost loss behaviour are being driven to some extent by coincident changes in regional hydro-climatic forcing mechanisms. Increases in annual air temperatures were observed at Fort Simpson during the 1990s, with the 1997/1998 ENSO period being the warmest. Similarly, elevated temperatures were experienced during the mid- to late-1990s at Norman Wells (Yi *et al.*, 2007) and in parts of Alaska (Osterkamp, 2007). Lara *et al.* (2016) found accelerating permafrost loss since 1998 within a plateau ecotone at Tanana Flats (Alaska) (average loss = 0.43% per year 1949–2009), while others (Camill, 2005; Smith *et al.*, 2005; Jorgenson *et al.*, 2006) found slight perturbations in depth of permafrost measurements also occurring at that time. These observations suggest that the trend of accelerated loss of permafrost following the 1997/1998 ENSO may be more geographically widespread than the northern boreal Taiga Plains.

While we cannot conclude which of the hydro-climatic drivers have the most influence on permafrost thaw (this would require long-term *in situ* monitoring), connections between drivers and permafrost loss after 1997/1998 can be demonstrated. In this study, we find a significant shift to greater snow accumulation during

the post-ENSO period (Table 1). While warmer temperatures have led to a later start to the snow-covered season by ~21 days on average (Fig. 3), early season snow accumulation increases more rapidly post-ENSO (~14% on average during 2000 period compared with 1970s). The impacts of snow on permafrost thaw are complex and depend in part on vegetation structure, accumulation amount, and timing of thaw (Osterkamp, 2007). However, the net effect of increased snow accumulation tends to insulate the ground surface from mid-winter extremes in low air temperatures, and further degrade permafrost beyond the seasonally thawed layer (e.g. Hinkel & Hurd, 2006; Osterkamp, 2007). Further, snow melt and earlier warming of snow-free near-surface permafrost enhances thaw (Wright *et al.*, 2008) via lateral movement of melt water, increased latent heat transfer and thermal conduction (Wright *et al.*, 2009). Based on a simple energy absorption scenario for reduced snow cover, plateau α decreased abruptly from 0.35 to ~0.09 associated with complete loss of snow (Helbig *et al.*, 2016a). The shortened snow-covered period of 35 days (on average) observed following the 1997/1998 ENSO and 50 days in 1998 within the SCW, results in an increase in total annual shortwave radiation absorption of 3% ($\pm 3\%$, Helbig *et al.*, 2016a) and 5% ($\pm 4\%$) per year. During the snow-free period, the increase in shortwave radiation absorption increases substantially by 12% ($\pm 0.7\%$) (with a reduction of 35 days) to 16% ($\pm 0.7\%$) (reduction of 50 days), respectively. Shortening of the snow-covered period (Fig. 3) combined with increased mid-winter snow pack insulation (Table 1) in the post-ENSO period therefore greatly increased the net radiant and sensible heat energy available for annual permafrost thaw.

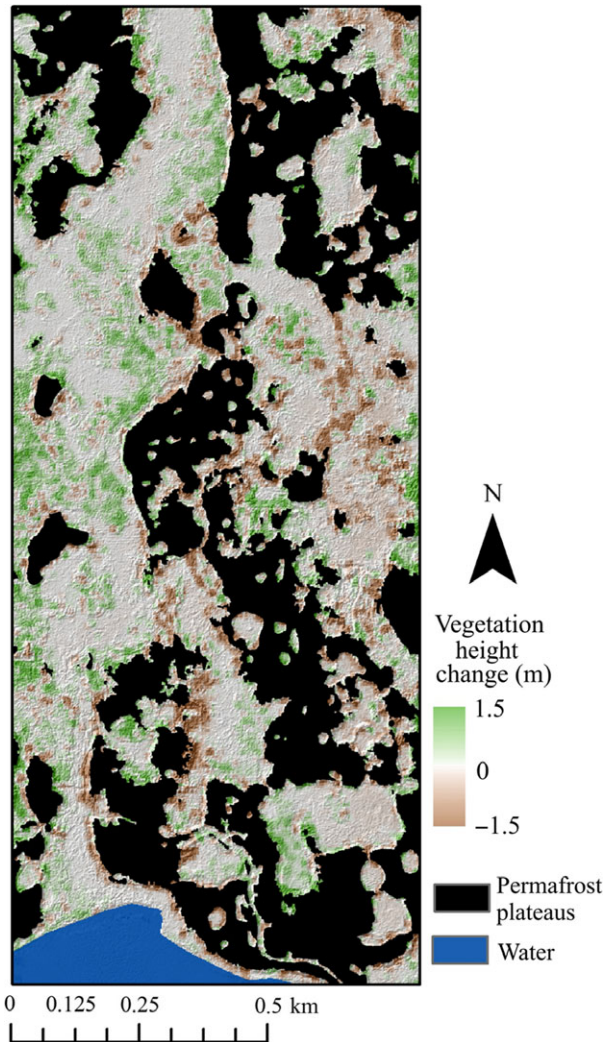


Fig. 7 Spatial variability of vegetation height change (2015 CHM-2008 CHM) within wetlands adjacent to plateaus within the LiDAR subset. Relatively small changes in plateau vegetation heights have been masked to illustrate changes in adjacent fen and bog environments.

The large change in the rate of permafrost loss that occurred around the time of the 1997/1998 ENSO is also associated with changing runoff behaviour. A shift in SCW hydrological response occurred immediately following the 1997/1998 ENSO as evidenced by the marked change in runoff ratio (Q/P) ($P = 0.0002$) and runoff (Q) ($P = 0.0001$) (Fig. 8). A significant change point in Q also occurs after the 1997/1998 ENSO for the adjacent Jean Marie ($P = 0.0001$), Birch ($P = 0.01$) and Trout River ($P = 0.02$) watersheds. This provides compelling evidence that the shift in watershed response at SCW occurred across the region.

Short-term exceptions to the rapid increase in Q/P occurred in 2012 and 2013, marked by substantial decreases in Q/P , despite the continued loss of permafrost observed from 2011 to 2015. During these two years, cumulative precipitation was within the 35th and 5th percentiles and Q was within the 25th and 3rd percentiles in 2012 and 2013, respectively, resulting in low Q/P . Reduced Q may be indicative of a short-term change in wetland storage during these two years and losses to evaporative fluxes following the warm year of 2011 (98th percentile). Rebound of Q/P in 2014 to 0.4 (slightly above the 1997–2015 average) occurred mainly as a result of above average runoff (64th percentile). Data following 2014 were not available for this study, so it is unknown at this point whether the dramatic shift in watershed runoff behaviour represents a long-term trend or a short-term response. In either case, the change in runoff ratio post-ENSO indicates either changes in watershed flow routing properties or changes in runoff input characteristics, or both.

Given the close temporal proximity to the terrain morphological and soil structural changes associated with post-ENSO accelerated permafrost loss, it follows that at least some of the change in runoff behaviour is due to increased watershed drainage efficiency. If indeed, drainage efficiency has increased, then some

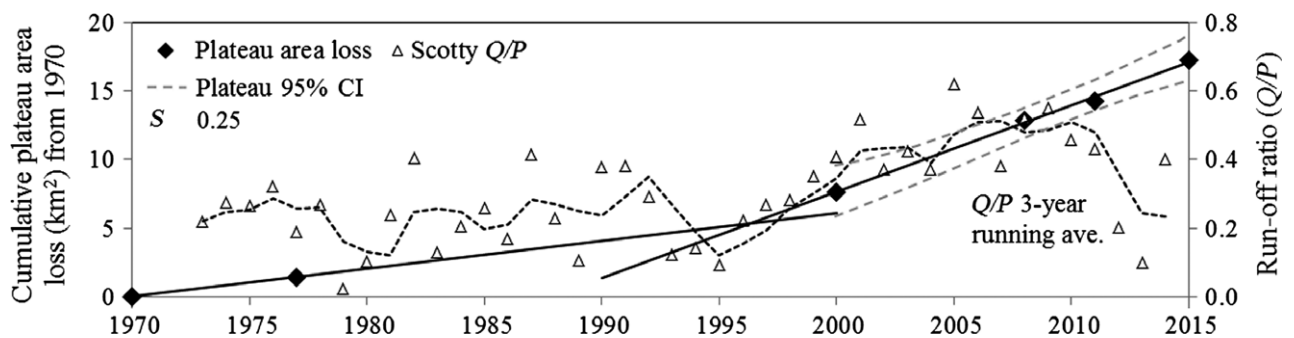


Fig. 8 Cumulative plateau area loss from 1970, scaled to the basin. Linear trends are forecast to 2000 and hindcast to 1990 to illustrate temporal correspondence between changing permafrost thaw and runoff ratio.

fraction of the increased runoff post-ENSO could be from long-term storage.

Two possibilities for long-term storage loss are considered: (i) regional groundwater; (ii) meltwater associated with long-term permafrost loss. We have no way to reasonably estimate changes in long-term groundwater storage for the entire SCW. However, it has been shown that the estimated volumetric contribution of observed permafrost losses to runoff is small and lies in the range of 0.6–6.4% (~1–10 mm) per year, with the likely true value nearer to the lower number. This is similar to an earlier estimate by Connon *et al.* (2014) who suggest 9 mm of contribution per year (with all surface losses extending to 10 m below ground).

Given the shift to increased Q/P cannot be explained by increased mobilization of water via permafrost loss (Fig. 4) or snow melt runoff (Table 1), it must indicate a change in drainage characteristics, which is congruent with physical morphological changes in the watershed due to permafrost loss. We therefore suggest that the anomalously warm air temperatures, shortened snow cover period, and timing of snow accumulation associated with the ENSO of 1997/1998 resulted in a tipping point that shifted the watershed into a new state. Increased connectivity as a result of fragmentation and loss of permafrost increases water flux to the basin outlet from wetland areas that were previously obstructed by permafrost plateaus (Connon *et al.*, 2014). Additional soil water input associated with thawing permafrost will enhance thermal erosion of plateau edges, accelerating fragmentation thereby increasing hydrological inputs from long-term storage (Quinton & Baltzer, 2013). In the short term, changes in drainage efficiency will have implications for basin storage (e.g. Velicogna *et al.*, 2012), larger peaks in runoff associated with P events, earlier downstream river ice break-up (Goulding *et al.*, 2009), and an increased probability for flooding of downstream communities (e.g. Prowse, 1986). Changes in long-term groundwater storage remain an unanswered question for the time being but if such losses exceed the rate at which they are replaced by rainfall, snow melt and permafrost thaw inputs, then it follows that some parts of this wetland dominated landscape could be gradually drying out.

Vegetation change and landscape evolution

Continued linear areal loss of permafrost observed since 1997/1998 is projected to result in a permafrost-free state by ~2044. If rate of loss of permafrost continues to a permafrost-free state, then this would be evidence that a tipping point had occurred resulting in a new ecological system. However, differential rates of loss observed along plateau edges (Fig. 5) indicate

areas where permafrost maintenance and decline vary spatially as a result of microclimatology (Sturm, 1992; Camill & Clark, 1998, 2000; Wright *et al.*, 2009; Quinton & Baltzer, 2013; Lara *et al.*, 2016). Previous studies have attempted similar observations using discrete field measurements; however, this requires extensive long-term monitoring, which is often challenging or not possible in remote northern areas. Gradual changes in forest mortality lagging permafrost loss may be observed in field measurements and historically through the use of optical imagery. Photogrammetric data sets are critical for examining long term, slow rates of change (e.g. Gamon *et al.*, 2012), whereas multitemporal LiDAR sampling allows the characterization of fine-scale changes in landscape structure. For wetland vegetation, spatially explicit observations of structural changes may provide evidence of landscape evolution processes, which can be challenging to observe using discrete field sampling or two-dimensional optical remote sensing methods. Field measurements of vegetation change depend on re-measurement of plots over a period of years. The efficacy of plot sampling can be constrained by accessibility issues and the possibility of inadvertent structural damage due to re-measurement over time (Cahill *et al.*, 2001). The fidelity of optical imagery and information occlusion from shadowing may also preclude identification of small changes in structure.

In this study, we observe slight growth and/or densification of woody vegetation species on north-east-facing slopes associated with areas of reduced permafrost thaw, while reduced height and canopy cover occurs with vegetation mortality along south-west margins (Fig. 6) (Camill & Clark, 1998). Additional field validation is required, especially along north-east plateau areas, to determine the nature of structural changes that have occurred in recent years. In other studies, Lara *et al.* (2016) found that black spruce trees continued to flourish within plateau interiors, linked to increased permafrost stability, while Baltzer *et al.* (2014) and Helbig *et al.* (2016b) found the opposite along saturated, thawing plateau margins.

Between 2008 and 2015, LiDAR observations illustrate both positive and negative changes in wetland vegetation canopy heights associated with locally elevated and depressed ground surface topography. Field measurements of Fafard (2014) (within a SCW rich fen) show an abundance of topographically elevated *Sphagnum fuscum* hummocks, lower water table, and shrub establishment. In this same fen, LiDAR-based change detection results illustrate vegetation growth of up to ~22 cm yr⁻¹ in some areas. Within other wetlands, topographically depressed areas are characterized by a higher local water table and are dominated by aquatic

plant communities (e.g. *Sphagnum* spp.). Further, woody vegetation/shrub growth exceeding 10 cm/yr occurs in wetland areas that are locally elevated and likely comparatively dry (e.g. Zoltai, 1993), thereby changing the local hydrological and energy balance characteristics of these shrub-wetland land covers (Blok *et al.* 2010). We find that increased shrub growth occurs on the western side of the fen (Fig. 7) adjacent to plateau edges that are predominantly north-east-facing, where rates of permafrost thaw are slightly reduced and plateaus are less fragmented by connected bogs and runoff channels (Fig. 5). It is likely that this part of the fen receives less runoff than the eastern side adjacent to rapid permafrost loss and connected bogs, but requires confirmation using field observations. Further, areas of vegetation mortality (deduced from canopy height loss from 2008 to 2015) within recently connected bogs may be indicative of changing drainage pathways and saturated soil conditions.

Patterns of topographically zonal vegetation changes in low relief wetland environments are evidence that water availability or excess and influences on water chemistry are driving these changes (e.g. Camill, 1999; Fafard, 2014). Given the fen and bog regions below plateaus represent low relief landscape elements, a shift from sedges to shrubs in areas of diminishing saturation will reduce local evaporation rates and increase transpiration, depending on shrub density/structure (Kettridge *et al.*, 2013), and shrub/moss species composition (Goetz & Price, 2016; Waddington *et al.*, 2015). Indeed, given the low gradients across the fens, vegetation zonation and associated changes may be equally or more important to the local hydrology than the surface drainage pathways.

Conceptual framework

In this study, we have shown that permafrost losses and watershed drainage efficiency increased dramatically and coincidentally following an anomalously warm ENSO in 1997/1998, with significant differences in hydro-climatic driving conditions pre- and post-ENSO. Increases in runoff ratio cannot be explained either by changes in precipitation magnitude or timing, or permafrost meltwater inputs, which leaves only reduced evaporative loss or increased groundwater drainage as possibilities to close the water balance. Reduced basin-wide evaporative loss appears an unlikely explanation for the discrepancy as it is opposite to what would be expected with increased air temperatures. However, if long-term net groundwater losses have occurred during the post-ENSO period, then the regional water table should drop resulting in increased resistance to evapotranspiration and a drying out of some wetland surfaces (Camill, 1999). Our observation

of net canopy growth over 7 years on elevated fen areas is compatible with a hypothesis of vegetation succession following the gradual drying out of peatland soils observed in other studies (e.g. Camill, 1999; Murphy *et al.*, 2009; Kettridge *et al.*, 2013) and reviewed in Waddington *et al.* (2015). The loss of biomass due to mortality around plateau edges in our small sample area appears to exceed (at least locally) the rate of canopy growth in adjacent fen areas. If permafrost plateaus continue to shrink at an accelerated rate, a point may soon be reached (if not already) where woody biomass growth exceeds mortality.

We contend that what we have observed in the combined remote sensing and hydro-climatic records represent active permafrost landscape evolution processes. Climatic drivers gradually moved the watershed towards a threshold state, where anomalous ENSO conditions led to a tipping point in the permafrost cover and drainage characteristics of the watershed resulting in changed hydrological behaviour including likely losses from long-term groundwater storage and changes to evaporative fluxes. The hypotheses described within this conceptual framework require further testing using integrated field, hydrometric and remote sensing data analysis.

Acknowledgements

We would like to acknowledge helpful, ongoing discussions with Drs. O. Sonnentag, W. Quinton, and Mr. M. Helbig and two anonymous reviewers. Early postdoctoral support (and invitation to work at SCW) of Chasmer was provided by SCW PI, Dr. W. Quinton. We would also like to thank Dr. Tristan Goulden and Ms. Allyson Fox for field and airborne survey support and data processing. LiDAR data were acquired in 2015 in collaboration with Teledyne Optech Inc., Toronto, Canada. Finally, important, long-term hydrometric and climate data records needed to monitor changes in hydro-climate were acquired from Water Survey of Canada and Environment Canada, respectively. Funding for this project was supported by the Campus Alberta Innovates Program, an NSERC Discovery Grant to Hopkinson, and Alberta Innovates Technology Futures to Chasmer.

References

- Baltzer JL, Veness T, Chasmer LE, Sniderhan AE, Quinton WL (2014) Forests on thawing permafrost: fragmentation, edge effects, and net forest loss. *Global Change Biology*, **20**, 824–834.
- Beilman DW, Robinson SD (2003) Peatland permafrost thaw and landform type along a climatic gradient. In: Proceedings of the 8th International Conference on Permafrost, Zurich. **1**, 61–65.
- Blok D, Heijmans MMPD, Schaepman-Strub G, Kononov AV, Maximov TC, Berndt F (2010) *Global Change Biology*, **16**, 1296–1305.
- Bonsal BR, Prowse TD (2003) Trends and variability in spring and autumn 0 C-isotherm dates over Canada. *Climatic Change*, **1**, 57–58.
- Bonsal B, Shabbar A (2011) Large-scale climate oscillations influencing Canada, 1900–2008. Canadian Biodiversity: Ecosystem Status and Trends 2010, Technical Thematic Report No. 4. Canadian Councils of Resource Ministers. Ottawa, ON iii + 15 pgs. Available at: <http://www.biodivcanada.ca/default.asp?lang=En&n=137E1147-0> (accessed 25 August 2016)

- Bonsal BR, Shabbar A, Higuera K (2001) Impacts of low frequency variability modes on Canadian winter temperature. *International Journal of Climatology*, **21**, 95–108.
- Cahill JF, Castelli JP, Casper BB (2001) The herbivory uncertainty principle: visiting plants can alter herbivory. *Ecology*, **82**, 307–312.
- Camill P (1999) Patterns of boreal permafrost peatland vegetation across environmental gradients sensitive to climate warming. *Canadian Journal of Botany*, **77**, 721–733.
- Camill P (2005) Permafrost thaw accelerates in boreal peatlands during late-20th century climate warming. *Climatic Change*, **68**, 135–152.
- Camill P, Clark JS (1998) Climate change disequilibrium of boreal permafrost peatlands caused by local processes. *The American Naturalist*, **151**, 207–222.
- Camill P, Clark JS (2000) Long-term perspectives on lagged ecosystem responses to climate change: permafrost in boreal peatlands and the grassland/woodland boundary. *Ecosystems*, **3**, 534–544.
- Chapin FS III, Eugster W, McFadden JP, Lynch AH, Walker DA (2000) Summer differences among Arctic ecosystems in regional climate forcing. *Journal of Climate*, **13**, 2002–2010.
- Chasmer L, Hopkinson C, Quinton W (2011) Quantifying errors in permafrost plateau change from optical data, Northwest Territories, Canada: 1947 to 2008. *Canadian Journal of Remote Sensing – CRSS Special Issue*, **36**, S211–S223.
- Chasmer L, Hopkinson C, Quinton W, Veness T, Baltzer J (2014) A decision-tree classification for low-lying complex land cover types within the zone of discontinuous permafrost. *Remote Sensing of Environment*, **143**, 73–84.
- Cannon RF, Quinton WL, Craig JR, Hayashi M (2014) Changing hydrologic connectivity due to permafrost thaw in the lower Liard River valley, NWT, Canada. *Hydrological Processes*, **28**, 4163–4178.
- DeBeer CM, Wheeler HS, Carey SK, Chun KP (2015) Recent climatic, cryospheric, and hydrological changes over the interior of Western Canada: a synthesis and review. *Hydrology and Earth System Sciences Discussions*, **12**, 8615–8674.
- Fafard M (2014) Musical chairs in a boreal peatland: how permafrost thaw reverses successional processes. Master's thesis. Wilfrid Laurier University. Paper 1637.
- Fleming SW, Whitfield PH (2010) Spatiotemporal mapping of ENSO and PDO surface meteorological signals in British Columbia, Yukon, and southeast Alaska. *Atmosphere-Ocean*, **48**, 122–131.
- Gamon JA, Kershaw GP, Williamson S, Hik DS (2012) Microtopographic patterns in an arctic baydjarakh field: do fine-grain patterns enforce landscape stability? *Environmental Research Letters*, **7**, 015502 (6 pgs).
- Gershunov A, Barnett TP (1998) Interdecadal modulation of ENSO teleconnections. *Bulletin of the American Meteorological Society*, **79**, 2715–2725.
- Goetz JD, Price JS (2016) Ecohydrological controls on water distribution and productivity of moss communities in western boreal peatlands, Canada. *Ecohydrology*, **9**, 138–152. doi:10.1002/eco.1620.
- Goetz SJ, Bunn AG, Fiske GJ, Houghton RA (2005) Satellite-observed photosynthetic trends across boreal North America associated with climate and fire disturbance. *Proceedings of the National Academy of Sciences of the United States of America*, **102**, 13521–13525.
- Goulding HL, Prowse TD, Beltaos S (2009) Spatial and temporal patterns of break-up and ice-jam flooding in the Mackenzie Delta, NWT. *Hydrological Processes*, **23**, 2654–2670.
- Government of the NWT (2016) Available at: <http://www.geomatics.gov.nt.ca/maps.aspx?i=5> (accessed 3 October 2016).
- Halsey LA, Vitt DH, Zoltai SC (1995) Disequilibrium response of permafrost in boreal continental western Canada to climate change. *Climatic Change*, **30**, 57–73.
- Hayashi M, Bentley LR, McClymont AF, Quinton WL (2009) Geophysical imaging of discontinuous permafrost: effects of sub-grid landcover variability and linear disturbance. *AGU Fall Meeting Abstracts*, **1**, 0449.
- Helbig M, Wischniewski K, Kljun N, Chasmer L, Quinton Q, Detto M, Sonnentag O (2016a) Permafrost disappearance impacts on near-surface climates of boreal forests. *Global Change Biology*. doi:10.1111/gcb.13348.
- Helbig M, Pappas C, Sonnentag O (2016b) Permafrost thaw and wildfire: equally important drivers of boreal tree cover changes in the Taiga Plains, Canada. *Geophysical Research Letters*, **43**, 1598–1606. doi:10.1002/2015GLD67193.
- Helbig M, Chasmer L, Kljun N, Quinton W, Treat C, Sonnentag O (in press). Increasing methane emissions cause a positive net radiative greenhouse gas forcing of a rapidly thawing boreal forest-wetland landscape. *Global Change Biology*. doi:10.1111/gcb.13520.
- Hinkel KM, Hurd JK (2006) Permafrost destabilization and thermokarst following snow fence installation, Barrow, Alaska, USA. *Arctic, Antarctic and Alpine Research*, **38**, 530–539.
- Hopkinson C, Chasmer L, Sass G, Creed I, Sitar M, Kalbfleisch W, Treitz P (2005) Vegetation class dependent errors in lidar ground elevation and canopy height estimates in a boreal wetland environment. *Canadian Journal of Remote Sensing*, **31**, 191–206.
- Hopkinson C, Chasmer L, Gynan C, Mahoney C, Sitar M (2016) Multi-sensor and multi-spectral lidar characterization and classification of a forest environment. *Canadian Journal of Remote Sensing - Special Issue on Advanced Forest Inventory*, **42**, 501–520.
- Hurrell JW (1996) Influence of variations in extratropical wintertime teleconnections on Northern Hemisphere temperature. *Geophysical Research Letters*, **23**, 665–668.
- de Jong R, Verbesselt J, Schaepman ME, Bruin S (2012) Trend changes in global greening and browning: contribution of short-term trends to longer-term change. *Global Change Biology*, **18**, 642–655.
- Jorgenson MT, Racine CH, Walters JC, Osterkamp TE (2001) Permafrost degradation and ecological changes associated with a warming climate in central Alaska. *Climatic Change*, **48**, 551–579.
- Jorgenson MT, Shur YL, Pullman ER (2006) Abrupt increase in permafrost degradation in Arctic Alaska. *Geophysical Research Letters*, **33**, L02503.
- Kettridge N, Thompson DK, Bombonato L, Turetsky MR, Benscoter BW, Waddington JM (2013) The ecohydrology of forested peatlands: simulating the effects of tree shading on moss evaporation and species composition. *Journal of Geophysical Research – Biogeosciences*, **118**, 422–435.
- Killick R, Fearnhead P, Eckley IA (2012) Optimal detection of changepoints with a linear computational cost. *Journal of the American Statistical Association*, **107**, 1590–1598.
- Lara MJ, McGuire AD, Euskirchen ES *et al.* (2015) Polygonal tundra geomorphological change in response to warming alters future CO₂ and CH₄ flux on the Barrow Peninsula. *Global Change Biology*, **21**, 1634–1651.
- Lara MJ, Genet H, McGuire AD *et al.* (2016) Thermokarst rates intensify due to climate change and forest fragmentation in an Alaskan boreal forest lowland. *Global Change Biology*, **22**, 816–829.
- Mantua NJ (2016) Available at: http://research.jisao.washington.edu/pdo/PDO_latest (accessed 3 August 2016).
- Mantua NJ, Hare SR, Zhang Y, Wallace JM, Francis RC (1997) A Pacific interdecadal climate oscillation with impacts on salmon production. *Bulletin of the American Meteorological Society*, **78**, 1069–1079.
- Meteorological Service of Canada (2016) Available at: <http://climate.weather.gc.ca/> (accessed 12 April 2016).
- Moore TR, Roulet NT, Waddington JM (1998) Uncertainty in predicting the effect of climatic change on the carbon cycling of Canadian peatlands. *Climatic Change*, **40**, 229–245.
- Murphy M, Laiho R, Moore T (2009) Effects of water table drawdown on root production and aboveground biomass in a boreal bog. *Ecosystems*, **12**, 1268–1282. doi:10.1007/s10021-009-9283-z.
- Natural Resources Canada (2011) A digital database of permafrost thickness in Canada. Natural Resources Canada, Ottawa, Ont. Available at: <http://geogratis.gc.ca/api/en/nrcan-mcan/ess-sst/91118544-1a57-5ea5-aa81-bd12465ea326.html> (accessed 7 October 2016).
- NOAA (2016) Available at: <http://www.cpc.ncep.noaa.gov/data/indices/soi> (accessed 3 August 2016).
- Osterkamp TE (2007) Characteristics of the recent warming of permafrost in Alaska. *Journal of Geophysical Research – Earth Surface*, **112**, F02S02. DOI: 10.1029/2006JF000578.
- Price DT, Alfaro RI, Brown KJ *et al.* (2013) Anticipating the consequences of climate change for Canada's boreal forest ecosystems 1. *Environmental Reviews*, **21**, 322–365.
- Prowse TD (1986) Ice jam characteristics, Liard-Mackenzie rivers confluence. *Canadian Journal of Civil Engineering*, **13**, 653–665.
- Quinton WL, Baltzer JL (2013) The active-layer hydrology of a peat plateau with thawing permafrost (Scotty Creek, Canada). *Hydrogeology Journal*, **21**, 201–220.
- Quinton WL, Hayashi M, Pietroniro A (2003) Connectivity and storage functions of channel fans and flat bogs in northern basins. *Hydrological Processes*, **17**, 3665–3684.
- Quinton WL, Hayashi M, Chasmer LE (2011) Permafrost-thaw-induced land-cover change in the Canadian subarctic: implications for water resources. *Hydrological Processes*, **25**, 152–158.
- Serreze MC, Walsh JE, Chapin FS *et al.* (2000) Observational evidence of recent change in the northern high-latitude environment. *Climatic Change*, **46**, 159–207.
- Shabbar A, Bonsal B (2003) An assessment of changes in winter cold and warm spells over Canada. *Natural Hazards*, **29**, 173–188.
- Smith SL, Burgess MM, Nixon FM (2001) Response of active-layer and permafrost temperatures to warming during 1998 in the Mackenzie Delta, Northwest Territories and at Canadian Forces Station Alert and Baker Lake Nunavut. Current Research 2001-E5 Natural Resources Canada.

- Smith SL, Burgess MM, Riseborough D, Nixon FM (2005) Recent trends from Canadian permafrost thermal monitoring network sites. *Permafrost and Periglacial Processes*, **16**, 19–30.
- St Jacques JM, Sauchyn DJ (2009) Increasing winter baseflow and mean annual streamflow from possible permafrost thawing in the Northwest Territories, Canada. *Geophysical Research Letters*, **36**, L01401.
- Stewart IT, Cayan DR, Dettinger MD (2005) Changes toward earlier streamflow timing across western North America. *Journal of Climate*, **18**, 1136–1155.
- Sturm M (1992) Snow distribution and heat flow in the Taiga. *Arctic and Alpine Research*, **24**, 145–152.
- Tarnocai C (2009) The impact of climate change on Canadian peatlands. *Canadian Water Resources Journal*, **34**, 453–466.
- Turetsky MR, Wieder RK, Vitt DH (2002) Boreal peatland C fluxes under varying permafrost regimes. *Soil Biology and Biochemistry*, **34**, 907–912.
- Velicogna I, Tong J, Zhang T, Kimball JS (2012) Increasing subsurface water storage in discontinuous permafrost areas of the Lena River basin, Eurasia, detected from GRACE. *Geophysical Research Letters*, **39**, L09403. DOI 10.2912/2012GL051623.
- Waddington JM, Morris PJ, Kettridge N, Granath G, Thompson DK, Moore PA (2015) Hydrological feedbacks in northern peatlands. *Ecology*, **96**, 113–127.
- Walvoord MA, Striegl RG (2007) Increased groundwater to stream discharge from permafrost thawing in the Yukon River basin: potential impacts on later export of carbon and nitrogen. *Geophysical Research Letters*, **34**, L12402, 12 pgs.
- Walvoord MA, Voss CI, Wellman TP (2012) Influence of permafrost distribution on groundwater flow in the context of climate-driven permafrost thaw: example from Yukon Flats Basin, Alaska, United States. *Water Resources Research*, **48**, W07524.
- Water Survey of Canada (2016) Available at: <https://wateroffice.ec.gc.ca/> (accessed 16 April 2016).
- Williams TJ, Quinton WL, Baltzer JL (2013) Linear disturbances on discontinuous permafrost: implications for thaw-induced changes to land cover and drainage patterns. *Environmental Research Letters*, **8**, 025006.
- Woo MK, Thorne R (2003) Streamflow in the Mackenzie basin, Canada. *Arctic*, **1**, 328–340.
- Wright N, Quinton WL, Hayashi M (2008) Hillslope run-off from an ice-cored peat plateau in a discontinuous permafrost basin, Northwest Territories, Canada. *Hydrological Processes*, **22**, 2816–2828.
- Wright N, Hayashi M, Quinton W (2009) Spatial and temporal variations in active layer thawing and their implication on runoff generation in peat-covered permafrost terrain. *Water Resources Research*, **45**, W05414.
- Yi S, Woo M-K, Arain MA (2007) Impacts of peat and vegetation on permafrost degradation under climate warming. *Geophysical Research Letters*, **34**, L16504.
- Zhang X, Vincent LA, Hogg WD, Niitsoo A (2000) Temperature and precipitation trends in Canada during the 20th century. *Atmosphere-Ocean*, **38**, 395–429.
- Zhang T, Barry RG, Knowles K, Ling F, Armstrong RL (2003) Distribution of seasonally and perennially frozen ground in the Northern Hemisphere. Proceedings of the 8th International Conference on Permafrost. 2, 1289–1294.
- Zoltai SC (1993) Cyclic development of permafrost in the peatlands of northwestern Alberta, Canada. *Arctic and Alpine Research*, **25**, 240–246.
- Zoltai SC, Tarnocai C (1971) Properties of a wooded palsa in northern Manitoba. *Arctic and Alpine Research*, **3**, 115–129.